CHEMICAL ENGINEERING TRANSACTIONS
VOL. 73, 2019
A publication of AIDIC
The Italian Association of Chemical Engineering
Online at www.aidic.it/cet
DOI: 10.3303/CET1973046
Guest Editors: Andrea D'Anna, Paolo Ciambelli, Carmelo Sunseri

ISBN 978-88-95608-70-9; **ISSN** 2283-9216

Pre-Treatment Processes Optimization for the Purification of Olive Mill Wastewater through a Pilot-Scale Membrane Plant

Srikanth Vuppala[a], Claudio Cianfrini[a], Marco Stoller*[b]

[a] University of Rome "La Sapienza", Dept. of Astronautics Electrical Energy Eng., Via Eudossiana 18, 00184 Rome, Italy
[b] University of Rome "La Sapienza", Dept. of Chemical Materials Environmental Eng., Via Eudossiana 18, 00184 Rome, Italy
marco.stoller@uniroma1.it

The reported work deals with the evaluation of two different pre-treatment processes performances for the purification of a real olive mill wastewater. The wastewater was from an oil mill placed in the South of Italy and presents high Chemical Oxygen Demand (COD), Total Organic Carbon (TOC) and phenols concentrations, besides other organic pollutants, an acid pH and brown colour. Therefore, this complex wastewater resulted in low- biodegradable and difficult to be treated by a solely process. To this aim, the present work will evaluate optimal operating parameters of coagulation-flocculation and photocatalysis pre-treatments to achieve suitable physical-chemical properties of the effluent, before the membrane treatment in a pilot-scale plant. In detail, the wastewater was firstly treated with an organic coagulant (chitosan) and then a photocatalytic step follows before the more efficient integrated membrane process. After the photocatalytic process, the COD, TOC and Phenols concentrations decreased to up 42 %, 38 % and 36 %, respectively, in comparison with the initial values. Subsequently, a series of four separation processes (ultrafiltration, nanofiltration and reverse osmosis) was performed and almost the total initial COD, TOC and phenols concentrations were removed.

1. Introduction

Wastewater treatment is a serious problem around the industrialized world (Vilardi, 2019), considering the remarkable industrial development of various countries (Bavasso et al., 2018), as well as the treatment of contaminated sites (Di Palma et al., 2007). The complexity of various wastewaters deriving from tannery (Vilardi et al., 2018a) and olive mill processes (Ochando-Pulido and Stoller, 2015) represents the real difficulty for operators and engineers when the most suitable combination of processes should be selected (Vilardi et al., 2018b). In particular, various problems have been raised in the last two decades for the treatment and disposal of olive mill wastewaters (OMW) (Paraskeva and Diamadopoulos 2006). About 2540000 t/year of olive oil is produced every year from all over the world from approximately 750 million productive olive trees and most of the production is in the Mediterranean region: indeed, this region alone produces 97% of the total olive oil production (Ochando-Pulido et al., 2014). In the process of olive oil production high amount of OMW is generated which induces environmental pollution, mainly associated with high organic concentration, phytotoxicity and biodegradation recalcitrance; for this reason, biological processes resulted in unsuccessfully (Di Palma and Verdone, 2009), as well as the use of bio-sorbent (Vilardi et al., 2018c). Therefore, the use of a suitable pre-treatment is necessary to achieve those physical-chemical characteristics required for its disposal in water bodies (Stoller et al., 2017a). The two main pre-treatments of OMW are represented by photocatalysis (Chinh et al., 2018) and coagulation-flocculation processes (Stoller et al., 2016). Various researchers successfully tested the use of metallic nanoparticles for the removal of various pollutants (Vilardi et al., 2017b), such as heavy metals (Gueye et al., 2016), metalloids (Vilardi et al., 2018d), organic compounds (Vilardi et al., 2018e) and inorganic anions (Muradova et al., 2016). The use of nanoparticles in various sectors, such as in civil (Di Palma et al., 2015), in the cosmetic (Stoller et al., 2017b), and in the environmental one (Vilardi et al., 2017a) has been extensively studied (Vilardi et al., 2019a), as demonstrated

Paper Received: 13 March 2018; Revised: 15 September 2018; Accepted: 19 December 2018

Please cite this article as: Vuppala S., Cianfrini C., Stoller M., 2019, Pre-treatment Processes Optimization for the Purification of Olive Mill Wastewater Through a Pilot-scale Membrane Plant , Chemical Engineering Transactions, 73, 271-276 DOI:10.3303/CET1973046

by the increasing number of publications on this field (Bavasso et al., 2016) and proved to be suitable to pre-treat complex wastewater such as OMW or tannery ones (Vilardi et al., 2019b).
The present work reports about the optimization of coagulation-flocculation and photocatalysis process for the pre-treatment of a real OMW from an olive mill placed in the South of Italy. Subsequently, the treated wastewater was processed using three membrane separation steps in series (ultra-filtration (UF), nano-filtration (NF) and reverse osmosis (RO)) (Stoller et al., 2018).

2. Materials and Methods

2.1 Materials

All the reagents were purchased from Sigma Aldrich (Milan) and were of analytical grade or higher. The solutions were prepared in deionized water. The following reagents were used in the experiments: chitosan, $FeCl_3 \cdot 6H_2O$, NH_4OH (33% v/v), HCl, Na_2SO_4, C_2H_5OH, $Si(OC_2H_5)_4$ and $Ti[OCH(CH_3)_2]_4$.

2.2 Coagulant preparation

5000 mg/L chitosan stock solution was prepared as follow: 500 mg of Chitosan 448877 from Sigma Aldrich (USA) was dissolved in 2.5 mL of 2 M HCl solution and 47.5 mL of deionized water; after 60 minutes, 50 mL of deionized water was added.

2.3 Nano-photocatalyst synthesis: Fe_3O_4-SiO_2/N-doped TiO_2 core-shell particles

The core-shell SiO_2/Fe_3O_4 nanoparticles (FM) were prepared by two steps. Firstly, Fe_3O_4 magnetic nanoparticles were synthesized using a spinning disk reactor (Vilardi et al., 2017c). Then, FM nanoparticles were prepared by dispersing Fe_3O_4 particles in distilled water, followed by the addition of C_2H_5OH (Sigma Aldrich). Tetraethyl Orthosilicate (TEOS), preliminarily diluted in C_2H_5OH, was added drop-wise to the Fe_3O_4 particle suspension. Then an aqueous solution of NH_3 (30 wt %) was added and the TEOS hydrolysis and condensation was allowed under overnight gentle stirring. The obtained FM particles were washed in a centrifuge using firstly water/ethanol mixtures then distilled water. Finally, they were dried and calcinated at 450 °C for 30 min (Ramp 10°C/min). Fe_3O_4-SiO_2/N-doped TiO_2 nanoparticles were prepared by adding urea in 50 mL water and stirred for 10 min, then Fe/SiO_2 was added in a sonicator for 5 min, further titanium tetraisopropoxide (TTIP) was added under sonication followed by 10 min of mechanical mixing. The mixture was centrifuged and washed two times. Subsequently, the recovered sample was calcinated at 450 °C for 30 min (Ramp 10°C/min) to obtain the final N-TiO_2/FM catalyst (Chinh et al., 2019). The nominal loading of N-TiO_2 on the FM support was 37.5 wt %.

2.4 Membrane processes

The sequence of membrane used in this work was ultrafiltration (UF, model GM supplied by GE Water), nanofiltration (NF, model DK supplied by GE Water) and reverse osmosis (RO, model SG supplied by GE Water), feeding the permeate stream of the previous separation step to the next one.

2.5 Experimental

The proposed process to treat OMW is started by treating through coagulation and flocculation, where gridding technique is used to separate coarse particles higher than the cut-size (300 μm) and then coagulation/flocculation experiments were carried on OMW samples by means of Jar test apparatus and putting 600 mL samples in 1 L beakers. Following the coagulant addition, the samples were subjected to a rapid mix step at 100 rpm for 2 min, a slow mixing step at 30 rpm for 30 min and subsequently a sedimentation step for 60 min. The chitosan coagulation process was optimized according to both coagulant dose and pH. Chitosan dosages in the range of 200 mg/L, 600 mg/L and 800 mg/L and pH values actual condition (4.6) and 3 pH were investigated to optimize the efficiency of coagulation and flocculation process, after coagulation and flocculation step, the created flocks in the OMW was settled out before continuing the treatment, performed by a 24 h long lasting sedimentation step. The sludge formed by this process was removed from the bottom of the tank. The best dosage and pH condition was chosen and proceeded for a large quantity for further treatment. The photocatalytic experiments were carried out with the first pre-treated OMW in coagulation method, at room temperature (25°C). The catalyst dosage was 1 g/L, 2 g/L and 3 g/L. The total OMW volume was 18 L. The experiments were conducted using a cylindrical photoreactor equipped with an air distributor device (Q_{air}=150 cm^3/min (STP)). Continuous mixing of the OMW was done by external recirculation of the same solution using a gear pump. The photoreactor was irradiated with a 25 Blue light LEDs (48 W nominal power; provided by New Oralight, with wavelength emission in the range 400–800 nm with a main emission peak at 475 nm. The system was left in the dark for 30 min to reach contaminants adsorption equilibrium, and then the photocatalytic reaction was initiated under visible light for 180 min,

according to the following time steps: 15, 30, 45, 60, 90, 120 and 180 min. After photocatalysis, the treated OMW which was separated from the catalyst by using magnet sent to the membrane treatment process. The boundary flux experiments were conducted by following Stoller and Ochando Pulido (2012) experimental procedure to evaluate the fouling phenomena, which could be possible to reduce fouling of membranes to do the separation of wastewaters. In this case, the analysis was constrained to the evaluation of irreversible fouling formation during operation by water flux measurements before and after the separation, after 15 min water rinsing. The residual concentration of Phenol, COD and TOC in aqueous samples was monitored by observing the change in the absorbance at the maximum absorption wavelength of 270 nm, 600 nm using a UV–vis spectrophotometer (UV-2700, SHIMADZU) and TOC analyser (TOC-L, SHIMADZU), then the concentrations were calculated from a calibration curve.

2.6 Mathematical modelling

The Phenols, TOC and COD variation monitored during photocatalysis tests were fitted to a pseudo-nth order kinetic model, expressed by the following equation:

$$X_t^{n-1} = \frac{X_0^{n-1}}{1 + (n-1)X_0^{n-1}kt} \quad (1)$$

where X is the specific parameter (Phenols, TOC or COD), n is the reaction order and k (M^{1-n}/min) is the kinetic constant. The non-linear regression of experimental data was accomplished in Excel environment, using the non-linear solver of Excel (Microsoft) to avoid the errors due to linearization procedure (Vilardi et al., 2018f). The experiments were conducted in duplicate and the mean values were reported. The percentage error was always below 4%.

3. Results and Discussion

3.1 Nanocatalyst samples characterization

Crystal phase composition and of N-TiO_2/FM were determined in previous work by XRD and RAMAN (Stoller et al., 2017c). XRD results of FM sample exhibited the presence of the orthorhombic phase of Fe_3O_4. From the XRD analysis spectra of N-TiO_2/FM compared with those of FM and unsupported N-TiO_2 powder, it was found the presence of the anatase-TiO_2 peaks with together the signals of FM. No diffraction peaks corresponding to SiO_2 were observed for FM and N-TiO_2/FM probably because silica has an amorphous structure. The same results were obtained from Raman analysis. Anatase and Fe_3O_4 crystallite size of the samples were evaluated from XRD analysis, using the Scherrer equation. For N-TiO_2, the anatase crystallite size was about 11 nm and slightly decreased (8 nm) after the deposition of N-TiO_2 on FM. Fe_3O_4 crystallite size was found to be about 20-26 nm which corresponds to the determined average particle size by SEM measurement (not shown). UV–vis reflectance spectra in terms of Reflectance for N-TiO_2. The shifting of the absorption onset from about 350 nm (for undoped TiO_2) to about 550 nm (for N-TiO_2) indicates the ability of the sample to absorb visible light, as confirmed by the band-gap energy (about 2.55 eV), which is the typical absorption property of TiO_2 doped with nitrogen.

3.2 Coagulation test

After gridding, the coagulation process was performed on the OMW. In detail, the following removal values were achieved according to the optimal pH=3 and chitosan concentration=600 mg/L: for Phenols, COD, TOC the removal efficiency was 22 %, 35 % and 28 % respectively. 600 mg/L of chitosan which was used for the coagulation and flocculation for the full scale of OMW quantity, after optimization based on the best results achieved. The supernatant was then processed by photocatalysis treatment.

3.3 Photocatalytic process

Preliminary experiments were carried out to verify that phenol, TOC and COD degradation by the heterogeneous photocatalytic process under visible light. It was found that in the absence of photocatalyst no decrease in phenol concentration was observed. Therefore, the photolysis phenomena did not occur. After 180 min of visible light irradiation, no photocatalytic activity was observed for the FM sample. On the contrary, N-TiO_2/FM catalysts was effective in the degradation of phenol, TOC and COD in aqueous solutions. The degradation of Phenols, COD and TOC in OMW is 38 %, 42 % and 36 % respectively. Figure 1 displays the experimental data fitted by the pseudo-nth order kinetic model.

As expected, the kinetic of COD removal was faster in comparison with those reported for TOC and Phenols, since the COD took into account also the oxidation of inorganic salts (Fe(II) to Fe(III) etc.) and usually the TOC and Phenols removal efficiency results lower than that reported for COD (Vilardi et al., 2018g). These considerations were validated by the higher n and k regressed value for COD removal kinetic (Table 1).

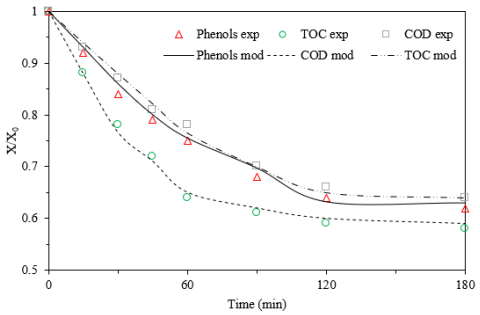

Figure 1: Phenols, TOC and COD removal kinetics and data fitting.

Table 1: regressed k and n values.

X	k (M^{1-n}/min)	n	R^2
COD	0.44	0.54	0.993
TOC	0.18	0.41	0.989
Phenols	0.152	0.41	0.988

Degradation efficiency decreased only at photocatalysis step, due to the OMW dark colour, and solid particles presence, which inhibits the photocatalytic efficiency of the treatment. Since the separability of photocatalysts from treated wastewater in a real wastewater treatment system is very important, magnetic N-TiO_2/FM sample was chosen for each treatment runs. The treated water containing N-TiO_2/FM catalyst was collected into a beaker after each treatment and the use of a magnet on the external surface of the beaker allows to easily separate the treated solution from the used photocatalyst. After washing with distilled water and drying at 105 °C, the photocatalyst was reused (data not shown) without further treatment. Supernatant collected from the photoreactor of catalyst dosage 3 g/L was chosen for the membrane treatment to continue the purification based on the results achieved in photocatalytic activity.

3.4 Membrane process

As expected, the suggested membrane processes in sequence reaches the foreseen targets in terms of purification of the wastewater stream (Figure 2).

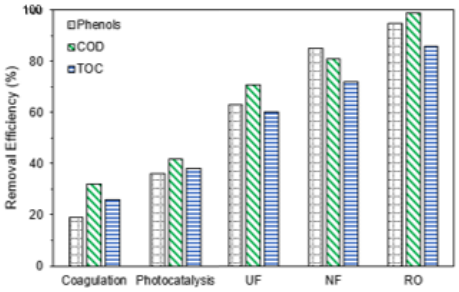

Figure 2: Degradation efficiency of each step of treatment.

The results obtained after the integrated treatment process were considerable if compared with the coagulation/photocatalysis process alone. In fact, after the first two processes, the degradation of Phenols, COD and TOC in OMW is 38 %, 42 % and 36 % respectively, was achieved. Indeed, a more efficient and complete organics removal could be reached only using a more powerful separation process, such as ultrafiltration and nanofiltration processes, that led to removing in the range of 86 to 99 % of Phenols, TOC and COD concentrations. Another important result was the pH variation at the end of the process; it passed from an acid value of 4.6 to a more neutral value of 7.2. This is an important feature, considering that after wastewater treatment, the effluent stream pH should be adjusted to the neutral value before its dispose of in water bodies. Concerning membrane fouling, the water permeability of the membrane was checked at the beginning of the experiment and at the end, after careful washing/rinsing. Table 2 reports the evaluation of the

operating conditions towards the boundary flux by adopting Chitosan (CTN), compared to those obtained by Stoller et al. (2017a) adopting as a pre-treatment acid flocculation and photocatalysis (AF+PC).

Table 2: Comparison of boundary fluxes as a function of different pre-treatments

Membrane	Boundary flux [L / (h m^2)]	
	CTN	AF+PC
UF	6.10	7.60
NF	12.50	14.90
RO	3.20	11.10

It is possible to observe that the membrane performances in terms of productivity by adopting the CTN procedure exhibit interesting values down to NF, whereas undergoing severe reduction at RO. This result may be justified by the same mechanism investigated previously by Stoller and Bravi (2010), where the presence of smaller particles, such as disaggregated chitosan, may trigger fouling issues on tighter membranes without affecting previous ones.

4. Conclusions

Coagulation tests were successfully performed using natural coagulant Chitosan for the degradation of pollutants in OMW. Nanocomposite N-TiO_2/SiO_2/Fe_3O_4 (N-TiO_2/FM), which are visible-active and magnetically separable, were synthesized successfully and tested in the photocatalytic removal of targeted pollutants under visible light irradiation. After an irradiation time of 180 min, the experimental results showed that N-TiO_2/FM nanoparticles are effective in the removal of phenol, COD and TOC reaching a value range of 36-42 % of removal efficiency. The removal process demonstrated to well follow pseudo-nth order kinetic model. Finally, the membrane treatment plant was employed to reach maximum degradation of Phenols, COD and TOC in the range of 86 to 99 % including pH reached up to 7.2 from an initial pH of OWM 4.6. The final COD was 0.5 g/L; it implies that an additional treatment is not necessary to discharge in to municipal sewer systems, whereas the Italian regulations with regards to the maximum COD allowed for liquid discharge in municipal sewer systems is equal to 500 mg/L or superficial aquifers equal to 125 mg/L. Concerning membrane fouling, chitosan pretreatment of OMW appears to be helpful in avoiding the phenomenon. Unfortunately, due to small particle blocking mechanisms, the appearance of severe fouling was observed on RO. As a consequence, this issue represents a technical constraint to the actual use of chitosan as a pretreatment step.

References

Bavasso I., Vilardi G., Stoller M., Chianese A., Di Palma L., 2016, Perspectives in Nanotechnology Based Innovative Applications for The Environment, Chemical Engineering Transactions, 47, 55–60.

Bavasso I., Montanaro D., Petrucci E., Di Palma L., 2018, Shortcut Biological Nitrogen Removal (SBNR) in an MFC anode chamber under microaerobic conditions: The effect of C/N ratio and kinetic study, Sustainability, 10, 1062-1075.

Chinh V.D., Broggi A., Di Palma L., Scarsella M., Speranza G., Vilardi G., Thang P.N., 2018, XPS Spectra Analysis of Ti2+, Ti3+ Ions and Dye Photodegradation Evaluation of Titania-Silica Mixed Oxide Nanoparticles, Journal of Electronic Materials, 47, 2215–2224.

Chinh V.D., Hung L.X., Di Palma L., Hanh V.T.H., Vilardi G., 2019, Effect of Carbon Nanotubes and Carbon Nanotubes/Gold Nanoparticles Composite on the Photocatalytic Activity of TiO2 and TiO2-SiO2, Chemical Engineering and Technology, 42, 308-315.

Di Palma L., Ferrantelli P., Merli C., Petrucci E., Pitzolu I., 2007, Influence of soil organic matter on copper extraction from contaminated soil, Soil and Sediment Contamination, 16, 323-335.

Di Palma L., Verdone N., 2009, The effect of disk rotational speed on oxygen transfer in rotating biological contactors, Bioresource Technology, 100, 1467-1470.

Di Palma L., Medici F., Vilardi G., 2015, Artificial aggregate from non metallic automotive shredder residue, Chemical Engineering Transactions, 43, 1723-1728.

Gueye M.T., Di Palma L., Allahverdeyeva G., Bavasso I., Petrucci E., Stoller M., Vilardi G., 2016, The influence of heavy metals and organic matter on hexavalent chromium reduction by nano zero valent iron in soil, Chemical Engineering Transactions, 47, 289-294.

Muradova G.G., Gadjieva S.R., Di Palma L., Vilardi G., 2016, Nitrates Removal by Bimetallic Nanoparticles in Water, Chemical Engineering Transactions, 47, 205–210.

Ochando-Pulido J.M., Stoller M., Di Palma L., Martinez-Ferez A., 2014, Threshold performance of a spiral-wound reverse osmosis membrane in the treatment of olive mill effluents from two-phase and three-phase extraction processes, Chemical Engineering and Processing, 83, 64–70.

Ochando-Pulido J.M., Stoller M., 2015, Kinetics and boundary flux optimization of integrated photocatalysis and ultrafiltration process for two-phase vegetation and olive washing wastewaters treatment, Chemical Engineering Journal, 279, 387–395.

Paraskeva P., Diamadopoulos E., 2006, Technologies for olive mill wastewater (OMW) treatment: a review, Journal of Chemical Technology & Biotechnology, 81, 1475–1485.

Stoller M., Bravi M., 2010, Critical flux analyses on differently pretreated olive vegetation waste water streams: some case studies, Desalination, 250, 578-582.

Stoller M., Ochando-Pulido J. M., 2012, Going from a critical flux concept to a threshold flux concept on membrane processes treating olive mill wastewater streams, Procedia Engineering, 44, 607-608

Stoller M., Azizova G., Mammadova A., Vilardi G., Di Palma L., Chianese A., 2016, Treatment of Olive Oil Processing Wastewater by Ultrafiltration, Nanofiltration, Reverse Osmosis and Biofiltration, Chemical Engineering Transactions, 47, 409–414.

Stoller M., Ochando-Pulido J.M., Vilardi G., Vuppala S., Bravi M., Verdone N., Di Palma L., 2017a, Technical and economic impact of photocatalysis as a pretreatment process step in olive mill wastewater treatment by membranes, Chemical Engineering Transactions, 57, 1171-1176.

Stoller M., Vilardi G., Di Palma L., Chianese A., Morganti P., 2017b, Process intensification techniques for the production of nanoparticles for the cosmetic and pharmaceutical industry, Journal of Applied Cosmetology, 35 (1-2), 53-59.

Stoller M., Sacco O., Vilardi G., Ochando-Pulido J.M., Di Palma L., 2018, Technical–economic evaluation of chromium recovery from tannery wastewater streams by means of membrane processes, Desalination and Water Treatment, 127, 57-63.

Vilardi G., Di Palma L., Verdone N., 2017a, Competitive Reaction Modelling in Aqueous Systems: the Case of Contemporary Reduction of Dichromates and Nitrates by nZVI, Chemical Engineering Transactions, 60, 175–180.

Vilardi G., Verdone N., Di Palma L., 2017b, The influence of nitrate on the reduction of hexavalent chromium by zero-valent iron nanoparticles in polluted wastewater, Desalination and Water Treatment, 86, 252–258.

Vilardi G., Stoller M., Verdone N., Di Palma L., 2017c, Production of nano Zero Valent Iron particles by means of a spinning disk reactor, Chemical Engineering Transactions, 57, 751–756.

Vilardi G., Di Palma L., Verdone N., 2018a, On the critical use of zero valent iron nanoparticles and Fenton processes for the treatment of tannery wastewater, Journal of Water Process Engineering, 22C, 109–122.

Vilardi G., Rodriguez-Rodriguez J., Ochando-Pulido J.M., Verdone N., Martinez-Ferez A., Di Palma L., 2018b, Large Laboratory-Plant application of a Tannery wastewater treatment by Fenton oxidation: Fe(II) and nZVI catalyst comparison and kinetic modelling, Process Safety and Environmental Protection, 117, 629-638.

Vilardi G., Di Palma L., Verdone N., 2018c, Heavy metals adsorption by banana peels micro-powder. Equilibrium modeling by non-linear models, Chinese Journal of Chemical Engineering, 26, 455-464.

Vilardi G., Mpouras T., Dermatas D., Verdone N., Polydera A., Di Palma L., 2018d, Nanomaterials application for heavy metals recovery from polluted water: the combination of nano zero-valent iron and carbon nanotubes. Competitive adsorption non-linear modeling, Chemosphere, 201, 716-729.

Vilardi G., Sebastiani D., Miliziano S., Verdone N., Di Palma L., 2018e, Heterogeneous nZVI-induced Fenton oxidation process to enhance biodegradability of excavation by-products, Chemical Engineering Journal, 335, 309–320.

Vilardi G., Ochando Pulido J.M., Verdone N., Stoller M., Di Palma L., 2018f, On the removal of Hexavalent Chromium by olive stones coated by iron-based nanoparticles: equilibrium study and Chromium recovery, Journal of Cleaner Production, 190, 200-210.

Vilardi G., Ochando Pulido J.M., Stoller M., Verdone N., Di Palma L., 2018g, Fenton oxidation and chromium recovery from tannery wastewater by means of iron-based coated biomass as heterogeneous catalyst in fixed-bed columns, Chemical Engineering Journal, 351, 1-11.

Vilardi G., 2019, Mathematical modelling of simultaneous nitrate and dissolved oxygen reduction by Cu-nZVI using a bi-component shrinking core model, Powder Technology, 343, 613-618.

Vilardi G., Di Palma L., Verdone N., 2019a, A physical-based interpretation of mechanism and kinetics of Cr(VI) reduction in aqueous solution by zero-valent iron nanoparticles, Chemosphere, 220, 590-599.

Vilardi G., Rodriguez-Rodriguez J., Ochando Pulido J.M., Di Palma L., Verdone N., 2019b, Fixed-bed reactor scale-up and modelling for Cr(VI) removal using nano iron-based coated biomass as packing material, Chemical Engineering Journal, 361, 990-998.